JOURNAL OF CATALYSIS 157, 592–602 (1995)

An Infrared Study of NO Decomposition over Cu-ZSM-5

Adam W. Aylor, Sarah C. Larsen, Jeffrey A. Reimer, and Alexis T. Bell

Materials Sciences Division, Lawrence Berkeley National Laboratory, and Department of Chemical Engineering, University of California, Berkeley, California 94720-1462

Received January 5, 1995; revised July 20, 1995; accepted July 21, 1995

The interactions of NO with Cu-ZSM-5 have been investigated by means of infrared spectroscopy. Following reduction by CO, most of the copper is present as Cu^+ cations. Room-temperature exposure of the reduced catalyst to NO results in the immediate appearance of $Cu^+(NO)$ and $Cu^+(NO)_2$. With time, these species disappear and are replaced by $Cu^{2+}(NO)$ and $Cu^{2+}(O^-)(NO)$. Evidence of the formation of $Cu^{2+}(NO_2)$ and $Cu^{2+}(NO_3^-)$ and of adsorbed N_2O and N_2O_3 is also observed. Similar species are observed upon room-temperature exposure of autoreduced and preoxidized Cu-ZSM-5. Above 573 K, the catalyst is active for NO decomposition to N_2 and N_2O. The selectivity to N_2 increases rapidly with increasing temperature and is essentially 100% at 773 K, the temperature at which the catalyst exhibits maximum activity. Infrared spectra taken under reaction conditions show weak peaks for $Cu^+(NO)$, $Cu^{2+}(O^-)(NO)$, and $Cu^{2+}(NO_3^-)$. With increasing temperature, the intensities of the peaks for $Cu^+(NO)$ and $Cu^{2+}(O^-)(NO)$ decrease but the proportion of the former species increases relative to the latter. Based on this evidence and rate data reported in the literature, a mechanism is proposed for the decomposition of NO. The first step in this mechanism is the formation of N_2O via the decomposition of $Cu^+(NO)_2$. N_2 is then formed via the reaction of N_2O with Cu^+ sites. O_2 formation is envisioned to proceed via the release of O atoms from $Cu^{2+}O^-$ and the subsequent reaction of O atoms with additional $Cu^{2+}O^-$ to produce $Cu^{2+}O_2^-$. The variation in the fraction of Cu^+ with temperature, deduced from the proposed mechanism, is in qualitative agreement with recent XANES observations. © 1995 Academic Press, Inc.

INTRODUCTION

Copper-exchanged ZSM-5 has been reported to have exceptionally high activity for the decomposition of NO to N_2 and O_2 (1–8). This observation has stimulated many studies aimed at identifying the nature of the active sites and the mechanism by which the reaction occurs. Investigations of catalyst structure have focused on determining the extent of copper dispersion within the zeolite and the oxidation state of the copper cations following oxidative or reductive pretreatment and during NO decomposition. Mechanistic deductions have been based to a large extent on observations of adsorbed species derived from infrared spectroscopy together with information drawn from kinetic and isotopic tracer experiments.

Electron paramagnetic resonance (EPR) studies demonstrate that immediately following exchange all of the copper is present as Cu^{2+}, presumably as a hydrated $Cu^{2+}(OH)^-$ species (7, 9). Heating freshly prepared Cu-ZSM-5 in flowing helium or in vacuum results in the autoreduction of Cu^{2+} to Cu^+ (7, 9, 10). This transformation has been observed directly by X-ray absorption near-edge structure (XANES) studies (11, 12) and has been inferred from EPR experiments (7, 9–15). The latter experiments suggest that the autoreduction process can be described by the reaction $2\ Cu^{2+}(OH)^- \rightleftharpoons Cu^+ + Cu^{2+}O^- + H_2O$, since all of the copper can be transformed back to Cu^{2+} by exposing an autoreduced sample of Cu-ZSM-5 to water vapor (9). XANES studies have shown that Cu^{2+} and Cu^+ coexist under reaction conditions and that the proportion of Cu^+ increases with the reaction temperature (11). Up to 773 K a linear correlation is observed between the rate of NO decomposition and the concentration of Cu^+, suggesting that Cu^+ participates in a redox mechanism during catalyzed NO decomposition. The siting and redox behavior of copper cations has also been investigated by Cu^+ photoluminescence (16, 17). These studies show that copper cations occupy two main sites; one in close proximity to two framework Al atoms and the other adjacent to one framework Al atom. The latter type of site is more prevalent in high Si/Al ratio ZSM-5 and increases on a relative basis with increasing Cu exchange level. Cu^{2+} cations associated with one framework Al atom are less readily reduced by CO or H_2 than those associated with two Al atoms. A linear correlation was established between the turnover frequency for NO decomposition and the concentration of Cu cations associated with one framework Al atom, suggesting that these Cu cations are the ones responsible for NO decomposition (17). More recently, EXAFS studies have shown that depending on the method of copper exchange, small clusters of copper oxide can form within the pores of the zeolite (12).

0021-9517/95 $12.00

Infrared investigations have revealed the coexistence of various adsorbed species (2, 10, 18–22). These include $Cu^+(NO)$, $Cu^+(NO)_2$, $Cu^{2+}(NO)$, and $Cu^{2+}(O^-)(NO)$, as well as adsorbed N_2O, NO_2, N_2O_3 and NO_3^-. In the case of the latter four species, the mode of interaction with copper cations is not identified explicitly. Exposure of Cu-ZSM-5 prepared in such a manner that all of the copper is present as Cu^+, or of an autoreduced sample of Cu-ZSM-5, results in the progressive disappearance of the bands associated with $Cu^+(NO)$ and $Cu^+(NO)_2$ and the concurrent growth of the bands associated with $Cu^{2+}(NO)$ [and/or $Cu^{2+}(O^-)(NO)$], as well as adsorbed NO_2 and NO_3^-. Many of the species associated with adsorbed NO and NO_2 are also observed when spectra are taken at temperatures between 623 and 723 K, where NO can undergo steady-state decomposition (21, 22).

Two principal views of the mechanism of NO decomposition have been advanced. The first is that $Cu^+(NO)_2$ decomposes, forming N_2O and leaving an oxygen atom behind (4, 15, 18, 19, 22). In this scheme the Cu^+ site is assumed to undergo oxidation to Cu^{2+}. The formation of N_2 is assumed to occur via the decomposition of N_2O. While this scheme provides an explanation for the formation of the N–N bond in N_2O and N_2, it leaves unanswered the question of how O_2 is formed and the means by which Cu^{2+} is reduced to Cu^+. Moreover, if the oxygen atom released in the decomposition of the dinitrosyl is assumed to remain as O^{2-}, then the issue of charge balance arises, since Cu^+ can only undergo a single-electron oxidation (21, 23). To address this difficulty, it has been proposed that a second reduced copper ion is required to furnish the second electron, resulting in the stabilization of O^{2-} as $[Cu^{2+}\text{-}O\text{-}Cu^{2+}]^{2+}$ (21, 23). More recently, it has been proposed that NO decomposition proceeds via a nitroso–nitrosyl complex, $Cu^{2+}(NO_2^-)(NO)$, which subsequently decomposes to produce N_2 and O_2 directly (21). The means by which the oxygen atom released in this process remains bound to the copper is not specified, but extra-lattice oxygen (ELO) is considered to be necessary for the reformation of the nitroso–nitrosyl complex via reaction with two molecules of NO. On the basis of isotopic exchange experiments, it has been proposed that the formation of O_2 cannot be assigned to identifiable ELO–copper ion ensembles, but it is rather a collective property of the copper-zeolite system (23). It is significant to note that the observed kinetics of NO decomposition, including the inhibition of NO decomposition by O_2, can be rationalized by both mechanisms, if appropriate assumptions are made (15, 21).

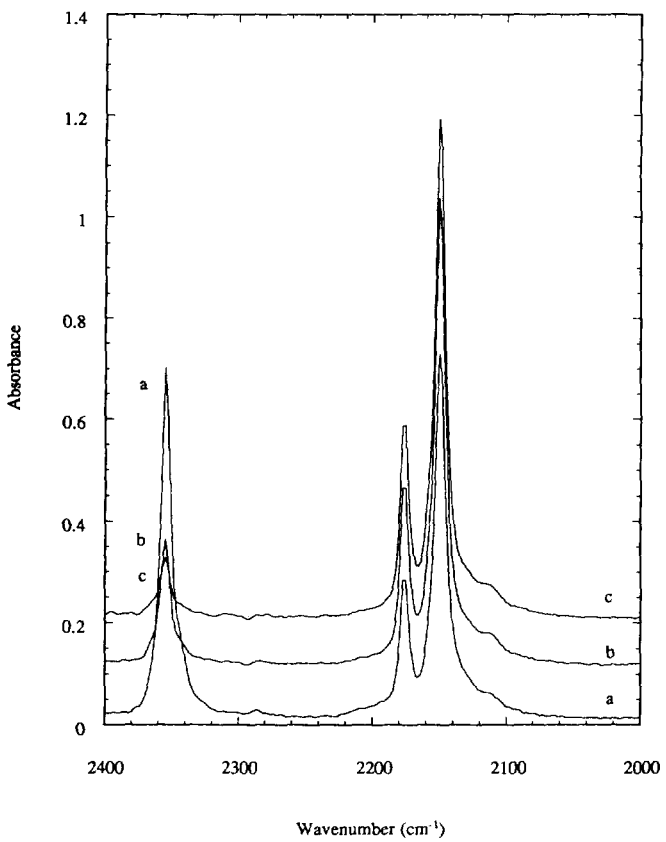

FIG. 1. Spectra of autoreduced Cu-ZSM-5 during room-temperature exposure to 4.21% CO for 1 min (a), 15 min (b), and 30 min (c).

The present investigation was undertaken with the aim of developing a clearer picture of the species adsorbed on Cu-ZSM-5 when it is exposed to NO, particularly under reaction conditions. It was of particular interest to determine the relative concentrations of various species during NO decomposition and to elucidate the extent to which copper is in an oxidized versus reduced state. To this end, infrared spectra were acquired for Cu-ZSM-5 exposed to NO, N_2O, NO_2, and N_2. Infrared spectra of adsorbed CO were used to characterize the catalyst following various types of pretreatment. Based on the accumulated evidence of this study, a detailed model for NO decomposition over Cu-ZSM-5 is proposed.

EXPERIMENTAL

ZSM-5 in the sodium form was synthesized by a template-free method (24, 25). NaOH (2.4 g) and $Al(OH)_3$ (1.2 g) were dissolved in 100 ml of distilled water and added slowly with stirring to 42.6 g of silica sol (Ludox 40%). Seed crystals of Na-ZSM-5 (0.14 g) were added to the gel to promote crystallization. The gel was heated at 453 K for 48 h in a Teflon-lined autoclave. The as-prepared zeolite crystals were washed with distilled water and dried overnight at 353 K. Copper exchange was performed using a dilute (0.1 *M*) solution of copper acetate. During the exchange the pH of the copper acetate solution was close to 7. From elemental analysis it is established that the Si/

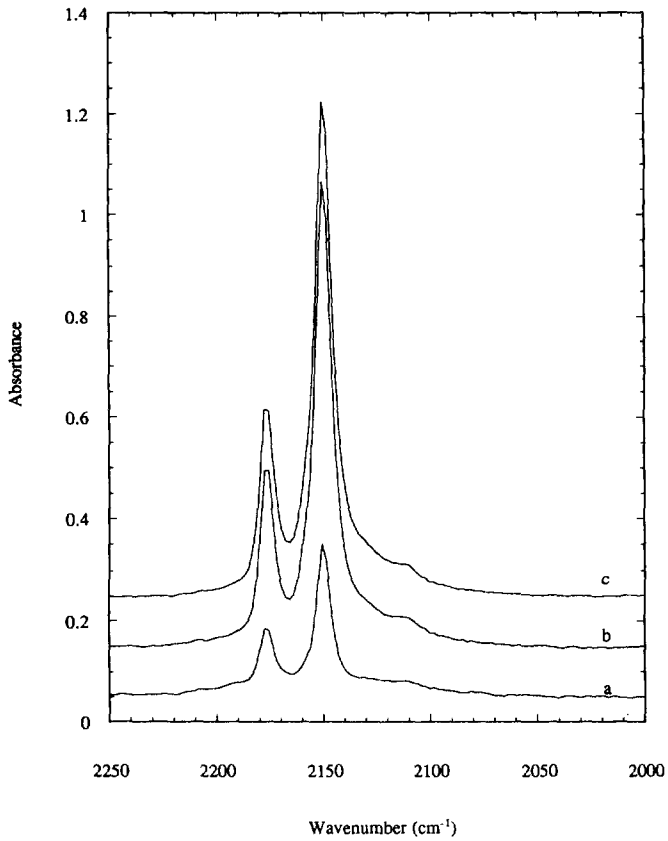

FIG. 2. Spectra of oxidized (a), autoreduced (b), and CO-reduced (c) Cu-ZSM-5 during room-temperature exposure to 4.21% CO for 15 min.

Al ratio of the zeolite is 18 and the percentage of Cu exchange is 92%.

For infrared spectroscopy, 10–20 mg of the zeolite was pressed into a self-supporting wafer and placed into an infrared cell similar to that described by Joly *et al.* (26). Spectra were recorded on a Digilab FTS-50 Fourier-transform infrared spectrometer at a resolution of 4 cm^{-1}. Typically, 64 scans were coadded to obtain a good signal-to-noise ratio. The spectrum of Cu-ZSM-5 in flowing He was subtracted from each spectrum.

Gases were supplied to the infrared cell from a gas manifold. NO (5%) in He and CO (4.21%) in He were obtained from Matheson. Oxygen and helium (UHP) were obtained on site. N_2O (10.3%) in argon was obtained from Matheson and N_2 was obtained on site. The effluent from the infrared cell was analyzed by infrared spectroscopy to determine the concentrations of NO, N_2O, and NO_2, and gas chromatography was used to determine the concentrations of N_2 and O_2. Infrared spectroscopy was carried out in a 10-cm pathlength gas cell. Chromatographic analyses were carried out with two Varian Model 3700 gas chromatographs connected in series. The first contained a Porapak Q column to separate N_2O from the remaining gases and the second chromatograph contained a column packed with 5-Å molecular sieve to separate NO, N_2, and O_2. NO_2 was removed from the gas stream in an ice bath located upstream of the first chromatograph to prevent permanent adsorption of NO_2 on the chromatographic columns.

Prior to each experiment the catalyst was pretreated in one of the following ways: (1) autoreduction—the catalyst is heated at 773 K in flowing He for at least 3 h and then cooled to the desired temperature; (2) oxidation—the catalyst is held in O_2 at 773 K for 1–3 h, then cooled to the desired temperature in O_2; or (3) reduction—the catalyst is heated in 4.21% CO at 773 K for 1–3 h then cooled in He to the desired temperature.

RESULTS

Interactions with CO

CO adsorption experiments were performed to probe the oxidation state of the catalyst following pretreatment. Figure 1 shows spectra taken as a function of time during the interaction of an autoreduced sample of Cu-ZSM-5 with CO at room temperature. Well-defined peaks are evident at 2150, 2177, and 2356 cm^{-1}, as well as a very weak band at 2115 cm^{-1}. With increasing time of exposure to CO, the peak at 2356 cm^{-1} decreases in intensity, while the pair of peaks at 2150 and 2177 cm^{-1} increases in intensity. Based on the recent work of Spoto *et al.* (19), the peaks at 2150 and 2177 cm^{-1} are assigned to the asymmetric and symmetric stretching vibrations of $Cu^+(CO)_2$. The small band at 2115 cm^{-1} may be due to CO that is bound through both the C and O ends to Lewis acid centers (27). The feature at 2356 cm^{-1} is assigned to weakly adsorbed CO_2 based on its proximity to the gas-phase value of 2349 cm^{-1}.

The appearance of CO_2 in the spectra shown in Fig. 1 is attributed to the removal of oxygen from the catalyst by CO. The simultaneous increase in the pair of bands for the dicarbonyl species and the decrease in intensity of the band for adsorbed CO_2 suggest the following reaction sequence:

$$Cu^{2+}O^- + CO \rightarrow Cu^+ + CO_2$$

$$Cu^+ + 2\,CO \rightarrow Cu^+(CO)_2.$$

Spectra of oxidized, autoreduced, and reduced Cu-ZSM-5 taken after 15 min of CO exposure at room temperature are shown in Fig. 2. The intensities of the pair of bands associated with dicarbonyl species are the same for the autoreduced and reduced samples. Since no change in the intensities of the dicarbonyl bands for the reduced sample was observed during CO exposure at room temperature, it is concluded that all of the $Cu^{2+}O^-$ is reduced to Cu^+ by exposure of the catalyst to CO at 773 K. The intensities

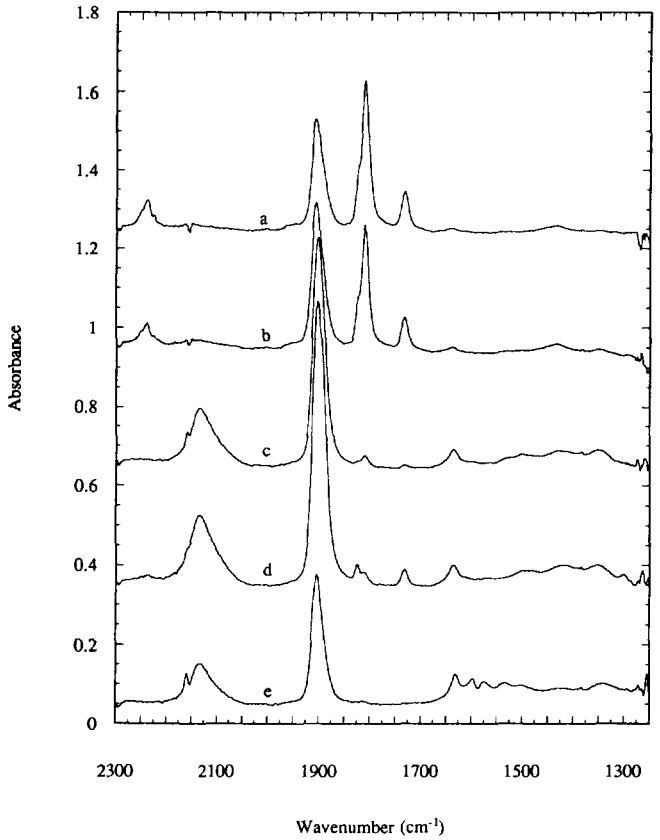

FIG. 3. Spectra of CO-reduced Cu-ZSM-5 during room-temperature exposure to 5870 ppm of NO for 1.5 min (a), 10 min (b), and 60 min (c), and after further exposure to 5% NO for 14 min (d) and subsequent purging in He for 5 min (e).

of the dicarbonyl bands for the oxidized sample are less intense than those for the reduced sample, indicating that after 15 min of exposure to CO, the oxidized sample is only partially reduced. This observation might be associated with the formation of cupric oxide species (e.g., small clusters of CuO_x) that undergo CO reduction more slowly than do $Cu^{2+}O^-$ produced by autoreduction. It is noted, though, that CO reduction of an oxidized sample of Cu-ZSM-5 in CO at elevated temperature and subsequent exposure to CO at room temperature produces a spectrum identical to spectrum c in Fig. 2.

While not shown, it was observed that upon flushing CO from the infrared cell at room temperature with He a residual band remained at 2157 cm^{-1}. This feature has been observed previously (10, 28) and is assigned to Cu^+CO.

Interactions with NO

Figure 3 shows a series of spectra taken during the exposure of a reduced sample of Cu-ZSM-5 to NO at room temperature. After 1.5 min of exposure, strong bands are observed at 1906 and 1810 cm^{-1}, together with weaker features at 2236, 1824, 1733, and 1633 cm^{-1}. Careful inspection and deconvolution of the band at 1906 cm^{-1} reveals that it is composed of two overlapping components centered at 1909 and 1895 cm^{-1}. A broad feature is also evident between 1550 and 1300 cm^{-1}.

On the basis of previous observations (8, 10, 18–21), the peak at 1810 cm^{-1} can be assigned to $Cu^+(NO)$ and the pair of peaks at 1824 and 1733 cm^{-1} can be assigned to $Cu^+(NO)_2$. The overlapping bands at 1895 and 1909 cm^{-1} are assigned to $Cu^{2+}O^-(NO)$ and $Cu^{2+}(NO)$, respectively (21). The former species is formed by the interactions of NO with $Cu^{2+}O^-$ and the latter species is formed by the interaction of NO with Cu^{2+} cations associated with $[-Al-O-Si-O-Al-]^{2-}$ structures in the zeolite framework. The peak at 2236 cm^{-1} is characteristic of adsorbed N_2O (29). The band observed at 1633 cm^{-1} is best assigned to a bidentate chelating nitrato-group (29). While the band at 1633 cm^{-1} has been assigned previously to NO_2 (21), this interpretation is inconsistent with reports that the highest frequency band for nitro- and nitrito-ligands associated with transition-metal complexes lie below 1475 cm^{-1} (29).

With increasing exposure of the sample to NO the band attributed to $Cu^{2+}O^-(NO)$ (1895 cm^{-1}) increases in inten-

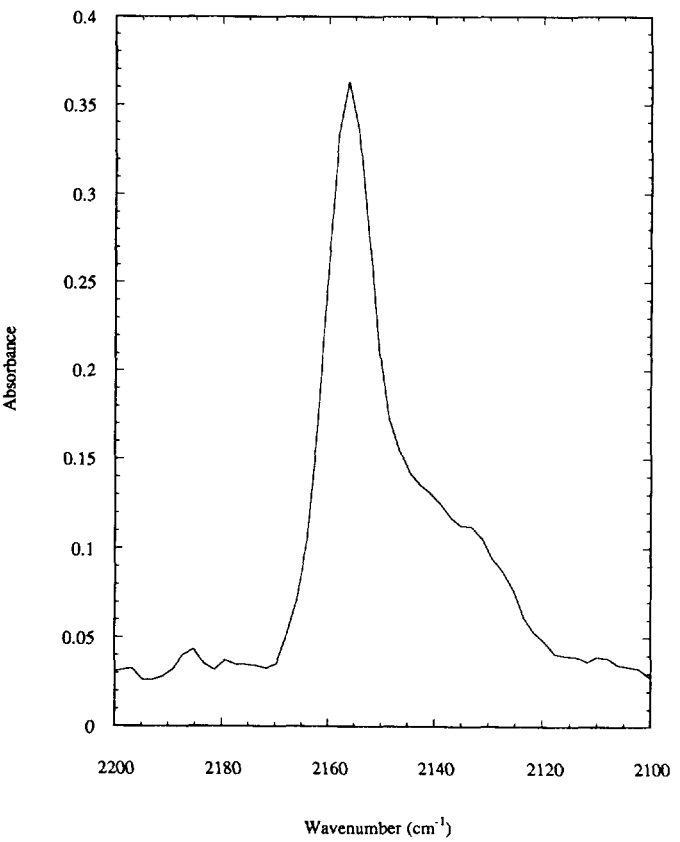

FIG. 4. Spectrum of autoreduced Cu-ZSM-5 exposed at room temperature to 1 atm of N_2.

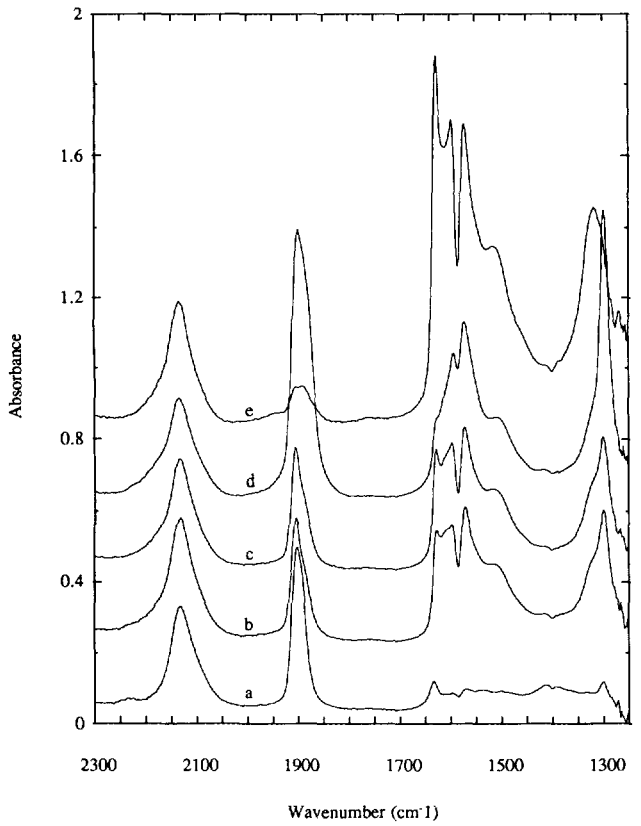

FIG. 5. Spectra of oxidized Cu-ZSM-5 during room-temperature exposure to 5870 ppm of NO for 1.5 min (a), 10 min (b), and 60 min (c), and further exposure to 5% NO for 14 min (d) and subsequent purging in He for 5 min (e).

sity as the intensity of the bands due to $Cu^+(NO)$ (1811 cm^{-1}) and $Cu^+(NO)_2$ (1824 and 1733 cm^{-1}) decrease in intensity; however, the intensity of the band at 1909 cm^{-1} is unaffected by the duration of NO exposure. These changes are accompanied by the disappearance of the band for N_2O (2236 cm^{-1}) and the appearance of a new band at 2133 cm^{-1}. When the exposure to NO is continued for 60 min a sharp band appears at 2156 cm^{-1}. This latter change is accompanied by a decrease in the intensity of the band for $Cu^{2+}(O^-)(NO)$ and the appearance of a series of overlapping bands between 1600 cm^{-1} and 1300 cm^{-1}.

Several investigators have previously reported the appearance of a band around 2130 cm^{-1} upon exposure of Cu-ZSM-5 to NO. Iwamoto *et al.* (7) and Giamello *et al.* (10) have attributed this band to $NO_2^{\delta+}$, but Valyon and Hall (21) have questioned this assignment on the basis of their observation that a band near 2130 cm^{-1} does not appear when Cu-ZSM-5 is exposed to NO_2. Very recently, Hoost *et al.* (30) have shown convincingly that a band observed at 2133 cm^{-1} upon adsorption of either NO or NO_2 can be attributed to NO_2^+ associated primarily with Brønsted acid sites. However, the authors leave open the possibility that some of the NO_2^+ may be associated with Cu^+ sites.

The band at 2156 cm^{-1} has been reported previously by Valyon and Hall (21) and assigned by them to adsorbed N_2. To confirm this assignment, an autoreduced sample of Cu-ZSM-5 was exposed to 1 atm N_2. Figure 4 shows that a well-defined feature is observed at 2156 cm^{-1}, together with a much less intense and broader feature at 2134 cm^{-1}. Both features disappear upon flushing of the cell with He, indicating that nitrogen is only weakly adsorbed.

The stability of the various features observed in the spectrum of adsorbed NO was determined by examining the effects of purging the infrared cell with He following exposure of the reduced sample to NO for 78 min. Spectrum e in Fig. 3 shows that the features associated with $Cu^+(NO)$, $Cu^+(NO)_2$, and $Cu^{2+}O^-(NO)$ disappear almost completely during the first few minutes of the He purge, indicating that molecularly adsorbed NO is weakly bound to both cuprous and cupric cations.

The interactions of NO with a preoxidized sample of Cu-ZSM-5 are illustrated in Fig. 5. After 1 min of NO exposure at room temperature bands are seen at 2133,

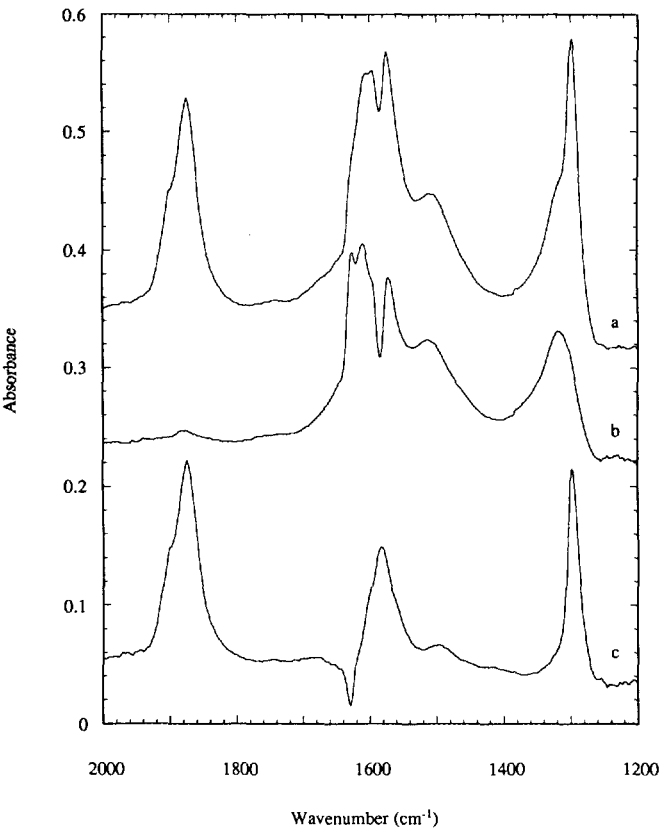

FIG. 6. Spectra of autoreduced Cu-ZSM-5 during exposure to 4.97% of NO for 10 min (following 58 min of exposure to 8625 ppm of NO) (a) and during subsequent He purging for 7 min (b). Spectrum (c) is the difference between spectra (a) and (b).

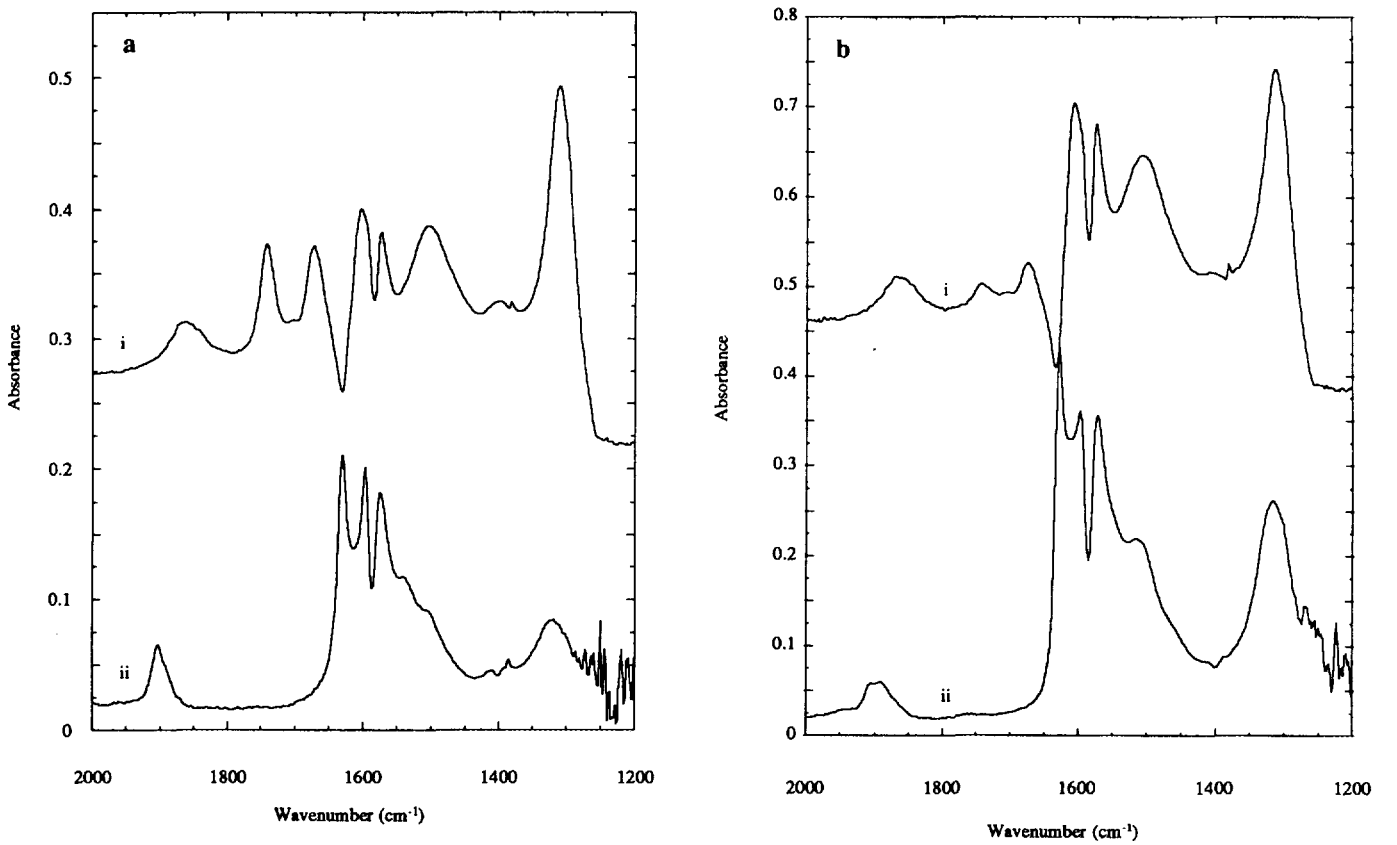

FIG. 7. (a) Spectrum of autoreduced Cu-ZSM-5 during room-temperature exposure to 1% NO_2 for 1 min (i) and during He purging following exposure to NO for 78 min (ii). (b) Spectrum of oxidized Cu-ZSM-5 during room-temperature exposure to 1% NO_2 for 4 min (i) and during He purging following exposure to NO for 56 min (ii).

1895, 1906, and 1633 cm^{-1}, together with a series of overlapping bands below 1600 cm^{-1}. With prolonged exposure to NO the spectrum of the oxidized sample exhibits an increase in the intensity of the band at 2133 cm^{-1} and the appearance of a series of bands below 1630 cm^{-1}. In this latter region maxima can now be clearly discerned at 1626, 1608, 1595, 1572, 1560, 1315, and 1298 cm^{-1}.

Strong evidence for the presence of N_2O_3 was obtained by subtracting the spectrum obtained after exposure of an autoreduced (or oxidized) sample to 5% NO from the spectrum obtained after subsequent purging of the sample in He. As shown in Fig. 6, well-defined bands located at 1876, 1578, and 1298 cm^{-1} are evident in the difference spectra. The positions of these bands agree very closely with those for solid-phase N_2O_3 (1863, 1589, and 1297 cm^{-1}) (29).

Spectra of NO_2 adsorbed on autoreduced and oxidized Cu-ZSM-5 are shown in Figs. 7a and 7b, respectively. For comparison, spectra of adsorbed NO are also shown. On the autoreduced sample, bands are clearly evident at 1862, 1740, 1673, 1607, 1600, 1572, 1500, and 1310 cm^{-1}. The bands at 1862 and 1572 are best assigned to N_2O_3 by comparison with the results presented in Fig. 6. The band at 1740 cm^{-1} is attributable to N_2O_4, whereas that at 1673 cm^{-1} is probably due to weakly adsorbed NO_2 (21, 29). The bands at 1607 and 1600 cm^{-1} are best assigned to bidentate nitrato-groups, and the band at 1500 cm^{-1} is best assigned to unidentate nitrato-groups, whereas the intense band at 1310 cm^{-1} may be due to a combination of nitrato- and nitro-groups (29). With prolonged exposure to NO_2 an additional band appears at 1349 cm^{-1}, characteristic of nitro-groups (29). The spectrum of NO_2 adsorbed on oxidized Cu-ZSM-5 is very similar to that for an autoreduced sample. The principal differences are that the bands at 1862, 1740, and 1773 cm^{-1} are less intense and those at 1607, 1600, and 1572 cm^{-1} are more intense. The spectra of NO adsorbed on autoreduced and oxidized Cu-ZSM-5 bear a number of similarities to those for adsorbed NO_2. The relative intensities of the bands suggest that NO tends to form bidentate nitrato-groups preferentially. It is also noted that the band at 1633 cm^{-1} observed in NO is absent from the spectrum taken in the presence of NO_2.

Spectra taken upon exposure of Cu-ZSM-5 to NO at progressively higher temperatures are shown in Figs. 8 and

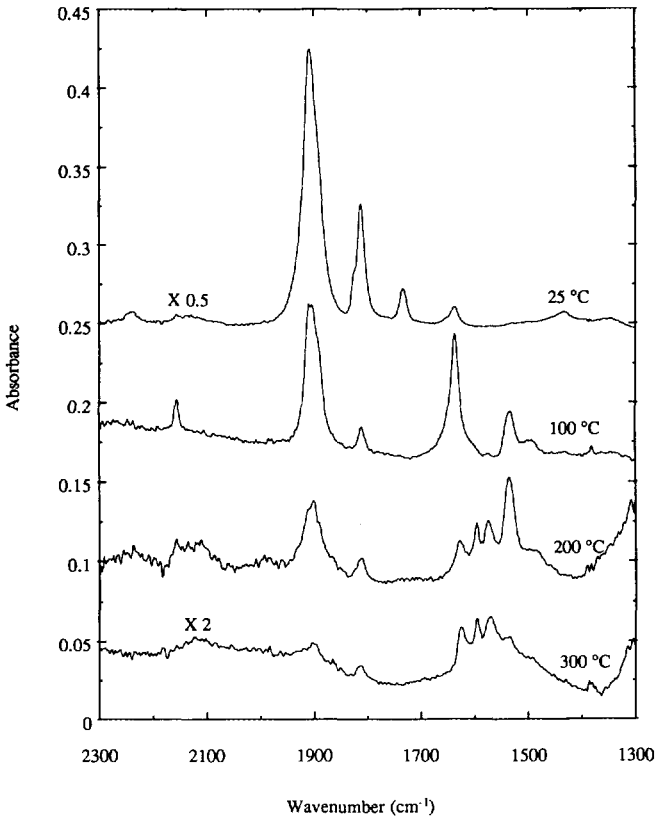

FIG. 8. Spectra during exposure of Cu-ZSM-5 to 6090 ppm of NO at progressively higher temperatures.

9. In the first of these figures the inlet concentration of NO is 6090 ppm (0.6%), whereas in the second it is 5%. With increasing temperature, the bands characteristic of $Cu^+(NO)$, $Cu^+(NO)_2$, $Cu^{2+}(O^-)(NO)$, and $Cu^{2+}(NO_2^-)$ are rapidly attenuated. The features located at 1630 cm^{-1} and below also decline in intensity with increasing temperature. Raising the NO concentration from 0.6 to 5% increases the intensity of the bands for adsorbed NO_3^- relative to those for NO and NO_2 at temperatures below 473 K. As noted below, the conversion of NO to N_2 and N_2O becomes significant only above 573 K. It is interesting to note, as well, that even at 573 and 673 K, small amounts of $Cu^+(NO)$ and $Cu^{2+}(O^-)(NO)$ can still be observed. Attention is called, as well, to the appearance of a small peak at 2156 cm^{-1}, readily observed at 373 K, due to N_2.

Figure 10 shows the conversion of NO to N_2 and N_2O as a function of temperature for an inlet feed concentration of 5% NO. The two principal products observed are N_2 and N_2O. All of the O_2 formed reacts with unconverted NO to produce NO_2 in the lines downstream from the reactor. As the reaction temperature increases above 573 K, the conversion of NO to N_2O passes through a broad maximum of 7% at about 650 K. By contrast, the conversion of N_2 increases to a maximum value of 32% at 823 K. The trends in both activity and product selectivity shown in Fig. 10 are comparable to those reported previously (10, 15).

DISCUSSION

A possible mechanism for explaining the decomposition of NO over Cu-ZSM-5 is presented in Fig. 11. The adsorption of NO occurs on both Cu^+ and $Cu^{2+}O^-$—the former resulting in the formation of $Cu^+(NO)$ and $Cu^+(NO)_2$ via reactions 1 and 2, respectively, and the latter in the formation of $Cu^{2+}(O^-)(NO)$ via reaction 4. The last of these species is thought to undergo rearrangement to produce a chelating bidentate $Cu^+(NO_2)$ species, reaction 5, which in the presence of NO reacts to form $Cu^+(N_2O_3)$, reaction 6. The latter reaction is readily reversible, as evidenced by the disappearance of the three bands for adsorbed N_2O_3 upon removal of gas-phase NO (see Fig. 6).

Gas-phase N_2O is formed by the decomposition of either $Cu^+(NO)_2$ or $Cu^+(N_2O_3)$. The first of these two paths, reaction 3, results in the formation of additional $Cu^{2+}(O^-)$, whereas the second path, reaction 7, results in the formation of $Cu^{2+}(O_2^-)$. N_2 is formed by the decomposition of N_2O via interaction with Cu^+ sites, reaction 8, whereas O_2 is formed by the decomposition of $Cu^{2+}(O_2^-)$, reaction 11. Decomposition of dinitrosyls to form N_2O is precedented in the field of organometallic chemistry [see, for example, Ref. (31)]. Further supporting this step is the observation of N_2O concurrent with the appearance of $Cu^+(NO)_2$ upon exposure of reduced or autoreduced Cu-ZSM-5 to NO at room temperature (32). The decomposition of $Cu^+(N_2O_3)$ to form N_2O and adsorbed O_2 has been proposed previously (33, 34), but no direct evidence for its occurrence has been presented. However, the possibility of this process occurring cannot be ruled out, since an estimate of the standard Gibbs free energies of decomposition for the reactions $N_2O_3 \rightleftharpoons NO_2 + NO$ and $N_2O_3 \rightleftharpoons N_2O + O_2$ reveal that the latter reaction is favored by 8.22 kcal/mol.

$Cu^{2+}O^-$ and $Cu^{2+}O_2^-$ are shown as product species resulting from the decomposition of NO. The first of these species has not been observed experimentally, but has been proposed as a product of the autoreduction of hydrated Cu-ZSM-5 (9). $Cu^{2+}O_2^-$ species have been reported in organometallic complexes, and the enthalpy for removal of oxygen as O_2 from such species is estimated to be about 8.5 kcal/mol (35).

The scheme presented in Fig. 11 envisages two possible paths by which N_2O might be formed, reactions 3 and 7. The first of these reactions is identical to that proposed earlier by Li and Hall (15), with the exception that the adsorbed oxygen atom is retained as $Cu^{2+}O^-$ rather than $[Cu^{2+} - O^{2-} - Cu^{2+}]^{2+}$. The second reaction is similar to that proposed by Spoto *et al.* (18, 19) and by Valyon and Hall (21), but differs in two respects. The first is that the adsorbed species undergoing decomposition is $Cu^+(N_2O_3)$,

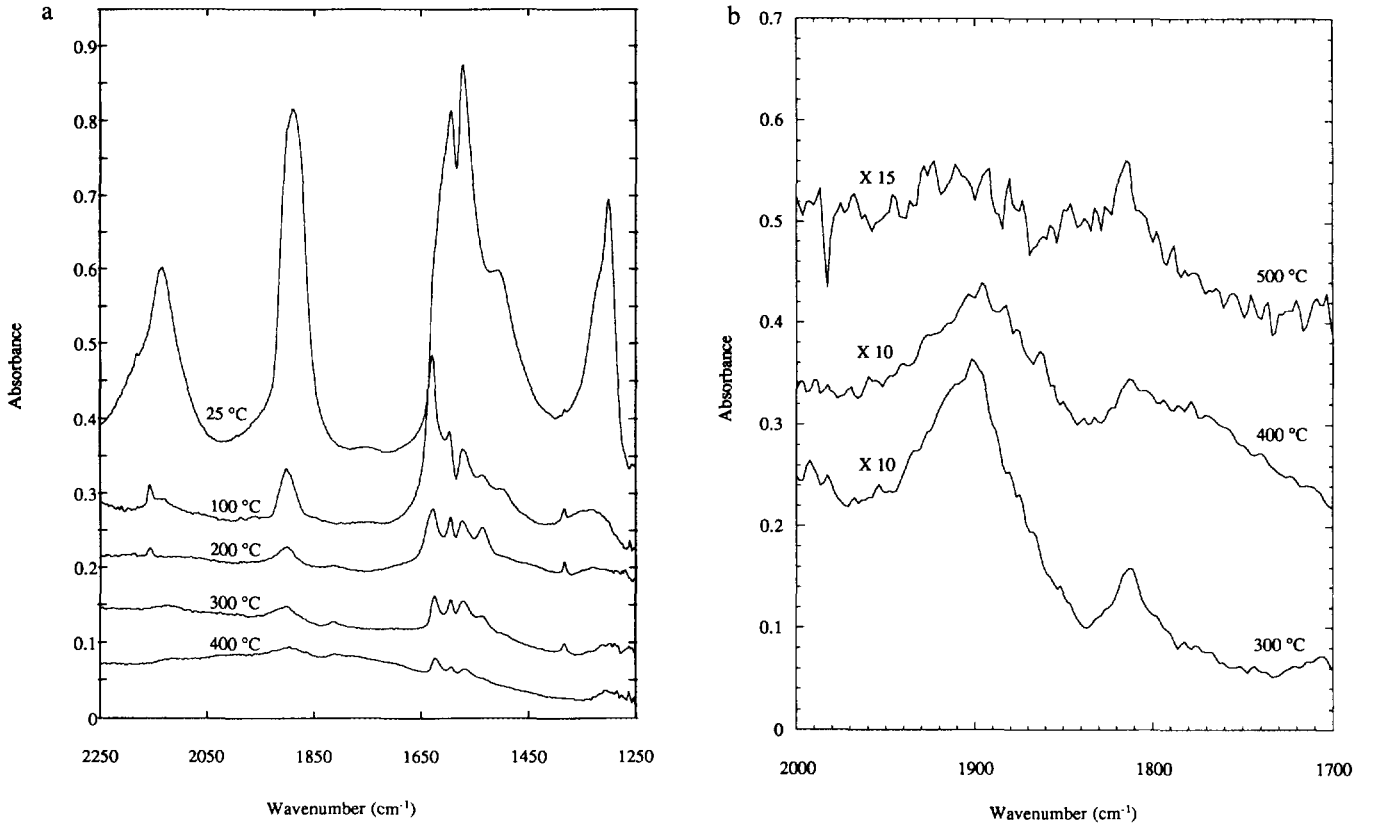

FIG. 9. (a) Spectra during exposure of Cu-ZSM-5 to 5% of NO at progressively higher temperatures. (b) A blowup of the region between 2000 and 1700 cm^{-1}.

rather than $Cu^{2+}(NO_2^-)(NO)$, and the second is that the decomposition products are N_2O and $Cu^{2+}(O_2^-)$, rather than N_2, O_2, and ELO. On the sole basis of infrared observations of the species present under reaction conditions it is not possible to determine whether reaction 3 or 7 is the dominant process for the decomposition of NO; however, one can develop an argument in favor of the first of these two processes by combining the results of infrared spectroscopy with those obtained from other techniques.

To begin with, we note that the fraction of Cu sites occupied by NO as $Cu^+(NO)$ or $Cu^{2+}(O^-)(NO)$ decreases dramatically as the temperature is raised. Figures 8 and 9 show that the intensity of the bands for these species decreases by a factor of over 60 as the temperature increases from 298 to 673 K. This means that at temperatures for which the conversion of NO is measurable, i.e., > 573 K, the fraction of Cu sites occupied by NO is of the order of 2% or less. The occupancy of Cu sites by NO_2^- and NO_3^- species also becomes small particularly when the partial pressure of NO is low (see Figs. 8 and 9). These observations suggest that during NO decomposition most of the Cu sites are present as Cu^+ or $Cu^{2+}O^-$.

Careful inspection of Figs. 8 and 9b shows that the ratio of the band intensities for nitrosyl vibrations in $Cu^+(NO)$ (ν_{NO} = 1810 cm^{-1}) and $Cu^{2+}(O^-)(NO)$ (ν_{NO} = 1895 cm^{-1}) increases with increasing temperature, suggesting that the ratio of Cu^+ to $Cu^{2+}O^-$ sites increases with temperature. This conclusion is consistent with observations of Cu-ZSM-5 by XANES during NO decomposition of a feed stream containing 1% NO (11). These experiments show that the fraction of Cu sites present as Cu^+ increases from 7.5 to 25% as the temperature increases from 573 to 773 K, the temperature at which the rate of NO decomposition reaches a maximum (11, 15). The increase in reduced Cu sites at elevated temperatures can be attributed to the release of oxygen via reactions 9–11.

If it is assumed that NO decomposition occurs predominantly via the decomposition of $Cu^+(NO)_2$ and that the rate of NO adsorption at Cu^+ sites is the rate-limiting step, it follows that the rate of NO decomposition will be first order in NO partial pressure. If it is further assumed that Cu cations are present predominantly as either Cu^+ or $Cu^{2+}O^-$ and that the stoichiometric reaction $Cu^{2+}O^- \rightleftharpoons Cu^+ + \frac{1}{2} O_2$ is at equilibrium, it can readily be shown that the rate of NO decomposition is given by

$$r = \frac{kC_{NO}}{(1 + KC_{O_2}^{1/2})}, \quad [1]$$

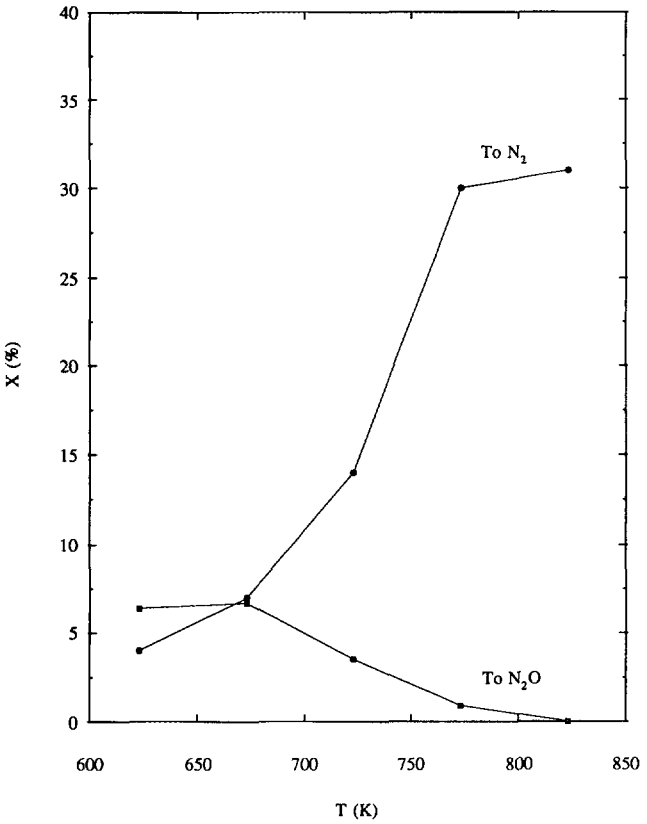

FIG. 10. NO conversion to N_2O and N_2 as a function of conversion. NO partial pressure, 38 Torr; catalyst weight, 0.15 g; total feed flowrate, 21 cm^3/min.

where k is an effective rate coefficient, K is the equilibrium constant for O_2 adsorption on Cu^+ sites, and C_{NO} and C_{O_2} are the gas-phase concentrations of NO and O_2, respectively. Equation [1] is identical to the rate expression presented by Li and Hall (15).

Under the assumptions used to derive Eq. [1], the fraction of Cu in the form of Cu^+ is given by

$$\theta_{Cu^+} = \frac{1}{(1 + K_{O_2}^{1/2})}. \qquad [2]$$

Since Li and Hall (15) have shown that the value of K decreases with increasing temperature consistent with an apparent heat of adsorption for O_2 of 26 kcal/mol of O_2, it follows that θ_{Cu^+} will increase with increasing temperature during an experiment in which a constant inlet concentration of NO is supplied to a reactor containing Cu-ZSM-5. This is exactly what was observed by Liu and Robota (11) by means of *in situ* XANES measurements of the proportion of Cu^+ present during NO decomposition.

Several factors argue against NO decomposition via either $Cu^{2+}(NO_2^-)(NO)$ or $Cu^+(N_2O_3)$. To begin with, there is no direct evidence for the first of these species. While $Cu^{2+}(N_2O_3)$ is observed at room temperature (see Fig. 6), this species readily decomposes at this temperature in the absence of gas-phase NO (see Fig. 6), and no evidence of this species is seen at higher temperatures, even in the presence of gas-phase NO (see Figs. 8 and 9). Valyon and Hall (21) have shown that the kinetics for NO decomposition reported by Li and Hall (15) can be rationalized by assuming that the adsorption of NO by an ELO-containing site (e.g., $Cu^{2+}O^-$) is the rate-limiting step and that N_2 is formed by the irreversible decomposition of $Cu^{2+}(NO_2^-)(NO)$. To account for the inhibition of NO decomposition by O_2, Valyon and Hall (21) assume the reaction $Cu^{2+}(NO_2^-) + \frac{1}{2}\,O_2 \rightleftharpoons Cu^{2+}(NO_3^-)$ to be at equilibrium and the Cu sites to be distributed between $Cu^{2+}O^-$, $Cu^{2+}(NO_2^-)$, and $Cu^{2+}(NO_3^-)$. However, as discussed above, this last assumption is inconsistent with the observation that only a small fraction, of order a few percent, of the Cu sites are occupied by NO_2^- or NO_3^- species under reaction conditions. Thus, here again, the progress of NO decomposition via an ELO-containing species does not seem to be supported by observation.

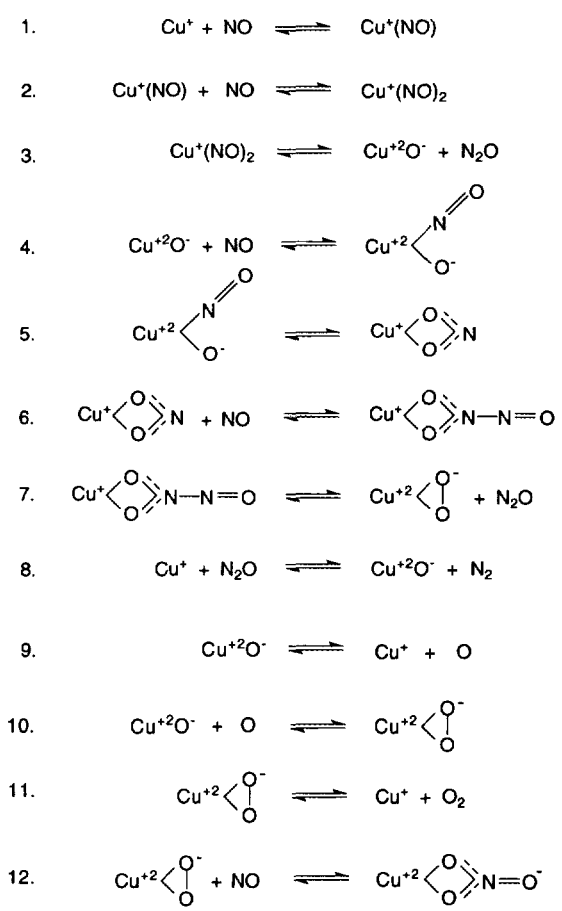

FIG. 11. Proposed mechanism for NO decomposition.

Hall and co-workers (36, 37) have reported that ^{18}O derived from either $^{18}O_2$ or $N^{18}O$ exchanges very rapidly with ELO at 773 K. On the basis of these observations they suggest a model for the formation of O_2 during NO decomposition, which envisages O atoms formed by NO decomposition entering the solid at reduced sites and then mixing with nearby lattice oxygen. O_2 is thought to be formed by a recombination of a lattice oxygen with an oxygen on an oxidized site. The mechanism of NO decomposition proposed in the present study provides an equally satisfying interpretation for these observations. O atoms released by desorption from $Cu^{2+}O^-$ can diffuse through the pores of the zeolite and react with either Si–OH present at defects in the lattice or Si–O–Si linkages in the zeolite framework. Such reaction will result in an exchange of O atoms between NO or O_2 and oxygen contained in the zeolite lattice.

CONCLUSIONS

Autoreduction of Cu-ZSM-5 results in the conversion of $Cu^{2+}(OH^-)$ species to a mixture of Cu^+ and $Cu^{2+}O^-$ species. The latter species can be reduced to Cu^+ by reaction with CO. Cu^+ cations react with NO at room temperature to form $Cu^+(NO)$ and $Cu^+(NO)_2$. With longer exposure to NO these species are converted to $Cu^{2+}(O^-)(NO)$, $Cu^{2+}(NO_2^-)$, and $Cu^{2+}(NO_3^-)$. Evidence of adsorbed N_2O and N_2O_3 is also observed. The catalyzed decomposition of NO to N_2 and N_2O is observed above 573 K. At 573 K the dominant product is N_2O, but with increasing temperature N_2 rapidly becomes the dominant product. Infrared spectra taken under reaction conditions show that only a small fraction of the copper sites contain adsorbate. NO is present exclusively as $Cu^+(NO)$ and $Cu^{2+}(O^-)(NO)$, with the former species predominating as the temperature increases. Small concentrations of $Cu^+(NO_3)$ are also observed.

The mechanism presented in Fig. 11 is proposed to explain the decomposition of NO over Cu-ZSM-5. Two pathways are envisioned for the formation of N_2O—one involving the decomposition of $Cu^+(NO)_2$ and the other the decomposition of $Cu^{2+}(N_2O_3^-)$. On the basis of the infrared observations reported in the present study and the kinetics of NO decomposition reported by Li and Hall (21), it is concluded that the first of these two pathways is dominant at elevated temperatures. N_2 is formed via the reaction of N_2O with Cu^+. O_2 is thought to form via a two-step process. O atoms first desorb from $Cu^{2+}O^-$ and then react with additional $Cu^{2+}O^-$ to produce $Cu^{2+}O_2^-$. The dependence of the fraction of copper cations present as Cu^+ on temperature under reaction conditions estimated from the rate parameters reported by Li and Hall (21) is in qualitative agreement with that reported by Liu and Robota (11) on the basis of XANES experiments.

ACKNOWLEDGMENTS

This work was supported by the Gas Research Institute under contract No. 5093-260-2492. S.L. acknowledges an appointment to the Distinguished Postdoctoral Research Program sponsored by the U.S. Department of Energy, Office of Science Education and Technical Information and Administered by the Oak Ridge Institute for Science and Education. The authors also thank Prof. Blanka Wichterlova for providing a preprint of Ref. (17).

REFERENCES

1. Iwamoto, M., Yoko, S., Sakai, K., and Kagawa, S., *J. Chem. Soc. Faraday Trans. 1* **77,** 1629 (1981).
2. Iwamoto, M., Furukawa, H., and Kagawa, S., *in* "New Developments in Zeolite Science and Technology" (Y. Murukama, A. Ichijima, and J. W. Ward, Eds.), p. 943. Elsevier, Amsterdam, 1986.
3. Li, Y., and Hall, W. K., *J. Phys. Chem.* **94,** 6145 (1990).
4. Iwamoto, M., and Hamada, H., *Catal. Today* **10,** 57 (1991).
5. Inui, T., Kojo, S., Shibata, M., Yoshida, and Iwamoto, S., *Stud. Surf. Sci. Catal.* **69,** 335 (1991).
6. Iwamoto, M., Yahiro, H., Tanada, K., Mozino, Y., Mine, Y., and Kagawa, S., *J. Phys. Chem.* **95,** 3727 (1991).
7. Iwamoto, M., Yahiro, H., Mizuno, N., Zhang, W.-X., Mine, Y., Furukawa, H., and Kagawa, S., *J. Phys. Chem.* **96,** 9360 (1992).
8. Teraoka, Y., Ogawa, H., Furukawa, and Kagawa, S., *Catal. Lett.* **12,** 361 (1992).
9. Larsen, S. C., Aylor, A. W., Bell, A. T., and Reimer, J. A., *J. Phys. Chem.* **98,** 11533 (1994).
10. Giamello, E., Murphy, D., Magnacca, G., Morterra, C., Shioya, Y., Nomura, T., and Anpo, M., *J. Catal.* **136,** 510 (1992).
11. Liu, D.-J., and Robota, H. J., *Catal. Lett.* **21,** 291 (1993).
12. Grunert, W., Hayes, N. W., Joyner, R. W., Shpiro, E. S., Siddiqui, M. R. H., and Baeva, G., *J. Phys. Chem.* **98,** 10832 (1994).
13. Centi, G., Perathoner, S., Shioya, Y., and Anpo, M., *Res. Chem. Interm.* **17,** 125 (1992).
14. Hamada, H., Matsubayashi, N., Shimada, H., Kintachi, Y. Ito, T., and Nishijima, A., *Catal. Lett.* **5,** 189 (1990).
15. Li, Y., and Hall, W. K., *J. Catal.* **129,** 202 (1991).
16. Dedecek, J., and Wichterlova, B., *J. Phys. Chem.* **98,** 5721 (1994).
17. Wichterlova, B., Dedecek, J., and Vondrova, A., *J. Phys. Chem.* **99,** 1065 (1995).
18. Spoto, G., Bordiga, S., Scarano, D., and Zecchina, A., *Catal. Lett.* **13,** 39 (1992).
19. Spoto, G., Zecchina, A., Bordiga, S., Ricchiardi, G., Martra, G., Loefanti, G., and Petrini, G., *Appl. Catal. B: Environ.* **3,** 151 (1994).
20. Valyon, J., and Hall, W. K., *in* "Proceedings, 10th International Congress on Catalysis, Budapest, 1992" (L. Guczi, F. Solymosi, and P. Tetenyi, Eds.), p. 1339. Elsevier, Amsterdam, 1993.
21. Valyon, J., and Hall, W. K., *J. Phys. Chem.* **97,** 1204 (1993).
22. Hall, W. K., and Valyon, J., *Catal. Lett.* **15,** 311 (1992).
23. Valyon, J., and Hall, W. K., *J. Catal.* **129,** 202 (1991).
24. Narita, E., Sato, K., and Taijiro, O., *Ind. Eng. Chem., Prod. Res. Dev.* **24,** 507 (1985).
25. Shiralkar, V. P., and Clearfied, A., *Zeolites* **9,** 363 (1989).
26. Joly, J. F., Zanier-Szyldowski, N., Colin, S., Raatz, F., Suaussy, J., and Lavalley, J. C., *Catal. Today* **9,** 31 (1991).
27. Bordiga, S., Platero, E. E., Arean, C. O., Lambert, C., and Zecchina, A., *J. Catal.* **137,** 179 (1992).
28. Sarkany, J., d'Itri, J. L., and Sachtler, W. H. M., *Catal. Lett.* **16,** 241 (1992).
29. Nakamoto, K., "Infrared and Raman Spectra of Inorganic and Coordination Compounds," 4th ed. Wiley-Interscience, New York, 1976.

30. Hoost, T. E., Laframboise, K. A., and Otto, K., *Catal. Lett.* **33,** 105 (1995).
31. Richter-Addo, G. B., and Legzdins, P., "Metal Nitrosyls." Oxford Univ. Press, Oxford, 1992.
32. Li, Y., and Armor, J. N., *Appl. Catal.* **76,** L1 (1991).
33. Chao, C.-C., and Lunsford, J. P., *J. Am. Chem. Soc.* **93,** 71 (1971).
34. Mastikhin, V. M., and Filimonova, S. V., *J. Chem. Soc. Faraday Trans.* **88,** 1473 (1992).
35. Karlin, K. D., Wei, N., Jung, B., Kaderli, S., Niklaus, P., and Zuberbuhler, A. D., *J. Am. Chem. Soc.* **115,** 9506 (1993).
36. Valyon, J., and Hall, W. K., *J. Catal.* **143,** 520 (1993).
37. Valyon, J., Millman, W. S., and Hall, W. K., *Catal. Lett.* **24,** 215 (1994).